The Distribution of Two-Phase R32 Over an Impacting T-Junction

Marijn Billiet*, Yves Bastien, Steven Lecompte, Lazova Marija, Alihan Kaya, Michel De Paepe
Department of Flow, Heat and Combustion Mechanics, Ghent University, Sint-Pietersnieuwstraat 41, 9000 Ghent, Belgium
*marijn.billiet@ugent.be

Abstract. This experimental work studies the distribution of a two-phase refrigerant flow over a horizontal impacting T-junction. A setup was built which consists of two parts: a flow conditioner and a test section. The flow conditioner creates a two-phase mixtures (R32) at a saturation temperature between $10\,^{\circ}\mathrm{C}$ and $20\,^{\circ}\mathrm{C}$ with a mass flux of 150 to $700\,\mathrm{kg}/(\mathrm{m}^2{\cdot}\mathrm{s})$ and a vapour quality between 0 and 1. In the test section, the two-phase flow is distributed over two identical parallel sections using an impacting T-junction. The backpressure and heat input of each parallel section can be regulated. The mass flow rates and vapour qualities are measured before and after the T-junction. Further, the pressure gradient over the T-junction is measured. Also the void fraction before the T-junction is determined using a capacitive void fraction sensor. Using design of experiments, the main effects of superficial vapour velocity, superficial liquid velocity and saturation pressure on the distribution of R32 were studied. For R32, the two phases only distribute uniformly over the T-junction when the mass flow rate through the two outlet branches is equal. Furthermore, the experiments show a decreased tendency of the liquid to exit through the outlet with the lowest mass flow rate with increasing superficial vapour velocity. The opposite is noticed with an increased superficial liquid velocity at a high superficial vapour velocity. Finally, no effect of the saturation pressure was found. The obtained results were then compared with the results of water-air mixtures found in literature.

Keywords: refrigerant, distribution, two-phase, heat pump

1. INTRODUCTION

Climate change is a major global concern. Heating and cooling of buildings contributes significantly to the climate change. Buildings are responsible for $36\,\%$ of all CO_2 emissions in the EU (European Commission, 2017). Therefore, the European Commission sets a target to decrease the emissions of buildings by $90\,\%$ by 2050. Besides improving the insulation of buildings, the current heating and cooling installations should be changed to ones that not depend on fossil fuels. A great example of this is a heat pump which can be powered by renewable energy.

A heat pump uses a thermodynamic cycle to upgrade low temperature heat to a higher temperature. The heat pump cycle consists of 4 components in a closed circuit: a compressor, a condensor, an expansion valve and a evaporator. The compressor compresses the gaseous refrigerant to a higher saturation pressure. In the condenser, the refrigerant condenses and high temperature heat is transfered to the application. The liquid refrigerant is then expanded over the expansion valve. Subsequently, the evaporator evaporates all the refrigerant by extracting heat from the environment.

When the refrigerant enters the evaporator, it is in the two-phase region. Furthermore, a typical evaporator consists of multiple parallel tubes. To distribute the two-phase flow over different parallel tubes a distributor is used. However, the distribution is often not homogeneous. Mader *et al.* (2015) showed that this maldistribution results in a significant drop in Coefficient Of Performance (COP) and capacity of the heat pump. Currently, little is known about the distribution of two-phase refrigerant flows in distributor heads. Some experimental studies aimed to improve the distributor head (Nakayama *et al.*, 2000; Yoshioka *et al.*, 2008). Both authors optimised the geometry of an existing distributor head using experimental techniques.

To better understand the phenomena behind the maldistribution, the distributor geometry in this work is reduced to an impacting T-junction. An impacting T-junction is a T-junction where both outlet branches are perpendicular to the inlet branch (Fig. 1). In literature, several authors investigated the distribution of water-air mixtures in impacting T-junctions (Azzopardi *et al.*, 1987; Hwang *et al.*, 1989; El-Shaboury *et al.*, 2007). The diameters used in literature ranged from $13.5\,\mathrm{mm}$ to $50\,\mathrm{mm}$ and all experiments were conducted at room temperature. Hong and Griston (1995) investigated impacting T-junctions with water-steam mixtures. A full overview of the literature can be found in Table 1. The superficial velocity J is the velocity of the phase assuming it occupies the complete section of the tube. The superficial velocity for the vapour (J_g) and liquid phase (J_l) is respectively given in Eq. (1) and 2.

$$J_g = \frac{\dot{m}_g}{\rho_g \cdot A} = \frac{G \cdot x}{\rho_g} \tag{1}$$

$$J_l = \frac{\dot{m}_l}{\rho_l \cdot A} = \frac{G \cdot (1-x)}{\rho_l} \tag{2}$$

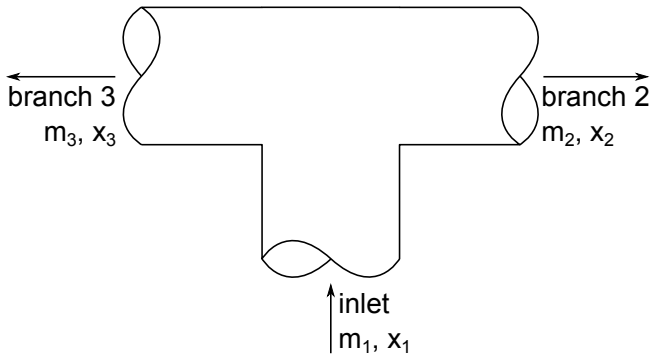

Figure 1: A schematic representation of the impacting T-junction. The flow enters in the inlet and is divided in the two branches.

Table 1: Experimental research of two-phase flow distribution in an impacting T-junction. (b = branch; i = inlet)

	Orientation$_i$	**Orientation$_b$**	**Mixture**	P_1 [bar]	**D** [mm]	$J_{g,i}$ [m/s]	$J_{l,i}$ [m/s]
Mohamed *et al.* (2014)	Horizontal	Horizontal	Air-water	1.5 - 2	13.5	2 - 40	0.01 - 0.18
Mohamed *et al.* (2011)	Horizontal	Inclined	Air-water	2	13.5	2 - 40	0.01 - 0.18
El-Shaboury *et al.* (2007)	Horizontal	Horizontal	Air-water	1.5	37.8	0.5 - 40	0.0026 - 0.18
Ottens *et al.* (1995)	Horizontal	Horizontal	Air-water	1	29.5	15.8	0.00063 - 0.03
Hong and Griston (1995)	Horizontal	Horizontal	Air-water	1	19	4.6 - 22.86	0.045 - 1.35
Chien and Rubel (1992)	Horizontal	Horizontal	Steam-water	28.6 - 42.4	49.3	12.2 - 33.5	0.082 - 1.74
Lightstone *et al.* (1991)	Horizontal	Horizontal	Air-water	1	20.0	0.1 - 2.65	0.01 - 0.18
Hwang *et al.* (1989)	Horizontal	Horizontal	Air-water	1.3 - 1.9	38	1.5 - 6.5	1.35 - 2.539
Azzopardi *et al.* (1987)	Vertical	Horizontal	Air-water	1.7	31.8	5.4 - 35.3	0.004 - 0.005

For the water-air mixtures, the above authors agree that the two phases only distribute uniformly over a horizontal impacting T-junction when the mass flow rate through the two outlet branches is equal. In all other cases, the phases have each a preference to flow through one of the outlet branches.

Further, all authors listed in Table 1 investigated the effects of the inlet superficial velocities ($J_{g,i}$ and $J_{l,i}$) on the phase distribution over an impacting T-junction. The authors varied one of the inlet superficial velocities while keeping the other one constant. For an horizontal impacting T-junction with horizontal branches all authors found the same trends. An increasing inlet superficial liquid velocity $J_{l,i}$ results in a increased tendency of the liquid to exit through the outlet with the lowest mass flow rate. The opposite effect was found for the inlet superficial vapour velocity. An increasing inlet superficial vapour velocity $J_{g,i}$ results in a decreased tendency of the liquid to exit through the outlet with the lowest mass flow rate. According to Mohamed *et al.* (2014), the phase with the lower rate of momentum will have an enlarged preference to exit through the outlet with the higher pressure gradient. The branch with the higher mass flow rate will have a larger pressure gradient. Hence the pressure just after the T-junction will be lower. Subsequently, a positive pressure gradient will be induced from the branch with the lowest mass flow rate to the one with the highest mass flow rate. The phase with the lowest rate of momentum will experience this pressure gradient as a driving force to flow to the branch with the largest flow rate.

Translated to the inlet vapour quality, this means when the inlet vapour quality increases, the vapour quality of the outlet with the lowest mass flow rate will be larger than the inlet vapour quality.

El-Shaboury *et al.* (2007) and Mohamed *et al.* (2014) investigated the effect of pressure on the phase distribution. Both concluded that the tendency of the liquid to exit through the outlet with the lowest mass flow rate decreases if the pressure in the system increases. An increase in pressure means an increase in air density, which increases the rate of momentum.

Mohamed *et al.* (2014) compared his data with the data of El-Shaboury *et al.* (2007) and found only a small effect of the tube diameter on the phase distribution. Increasing the tube diameter results in a very small increased tendency of the liquid to exit through the outlet with the lowest mass flow rate.

Finally, El-Shaboury *et al.* (2007) also found a dependency of the flow pattern. The authors observed a discontinuity in the trends of the superficial velocity effect between wavy and annular flow.

This work investigates if the results found for air-water mixtures are also applicable for refrigerants.

2. EXPERIMENTAL SETUP

The experimental setup is designed to measure the distribution of two-phase refrigerants (R32, R410a, R1234ze, R1234yf) over an impacting T-or Y-junction. A simplified representation of the experimental setup is shown in Fig. 2.

The experimental setup consists of two main parts: the test section and the flow conditioner. The flow conditioner creates a two-phase refrigerant flow with a given mass flux G ($150\,\mathrm{kg/(m^2{\cdot}s)}$ - $700\,\mathrm{kg/(m^2{\cdot}s)}$), saturation temperature ($10\,^\circ\mathrm{C}$ - $20\,^\circ\mathrm{C}$) and vapour quality x (0 - 1) which is fed to the test section. The test section simulates an evaporator of a typical heat pump. Both the test section and the flow conditioner are constructed with $3/8\,\mathrm{inch}$ copper refrigerant tubing which has an inner diameter of $8.0\,\mathrm{mm}$.

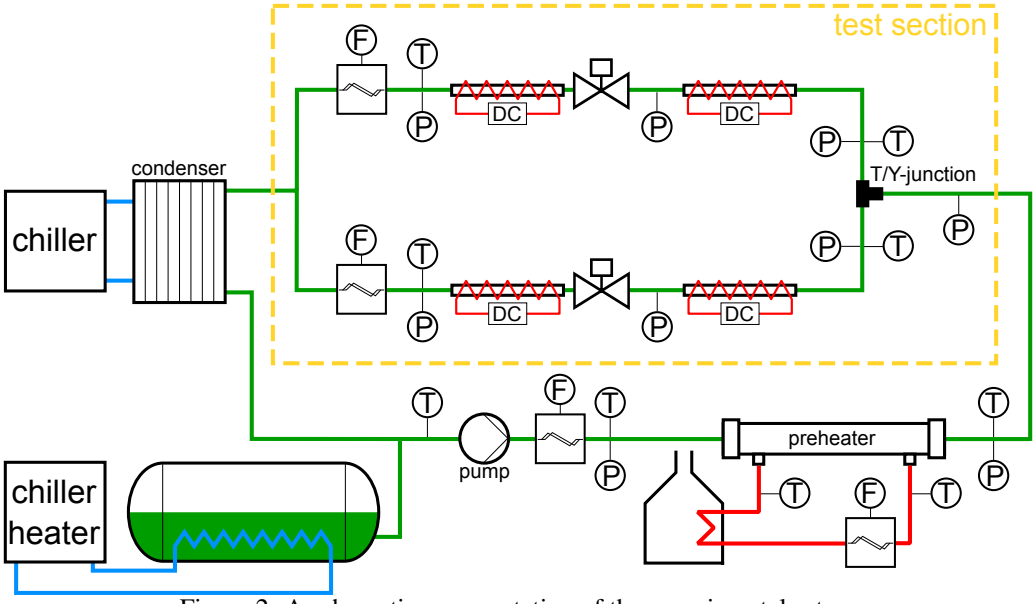

Figure 2: A schematic representation of the experimental setup.

The flow conditioner consists of a buffer vessel, a pump, a preheater, a condenser and specific measurement equipment. The buffer vessel, located on the bottom left of Fig. 2, is used to regulate the saturation pressure inside the experimental setup. The pressure is controlled by varying the temperature of the refrigerant in the vessel. The condenser is used to condensate and subcool the refrigerant coming from the test section. The condenser is a plate heat exchanger cooled by an external glycol circuit. The subcooled liquid refrigerant is pumped through a Coriolis mass flow meter (Bronkhorst Coriflow M55) to determine the mass flow rate of the refrigerant. The pump only compensates for the pressure drop over the tubing in the experimental setup. The subcooled refrigerant than passes through the preheater which is a modular tube-in-tube heat exchanger. The length of the heat exchanger can be varied between $1\,\mathrm{m}$ and $15\,\mathrm{m}$ in steps of $1\,\mathrm{m}$. The preheater uses hot water produced by a gas-fired boiler to heat up and evaporate the refrigerant to a certain vapour quality. After the preheater, the void fraction and flow regime is determined using an in-house made void fraction sensor (De Kerpel *et al.*, 2014, 2015).

The test section consists of a T- or Y-junction and two identical parallel circuits. The pressure drop over the junction is measured using a multiplexed differential pressure sensor (EH Deltabar S PMD75). Each parallel circuit contains an evaporator, a needle valve, a superheater and some instrumentation. The back pressure of a circuit can be regulated using the needle valve or by adjusting the heat flux of the evaporator. The superheater ensures that the refrigerant is superheated when entering the Coriolis mass flow meter (Krohne Optimass 6000 S10) which is required for proper functioning of the meter. Both the evaporator and superheater are electrical heaters wrapped around the copper tube. The maximum power of the evaporator and superheater is respectively $3\,\mathrm{kW}$ and $600\,\mathrm{W}$. These electrical heaters are fed by computer controlled DC power supplies. The test section can also be rotated over a range of $90°$ which enables different orientations of the T-junction. All the temperature measurements are conducted by K-type thermocouples which are read out by a *Keithley 2700*. The thermocouples were calibrated using a dry-block calibrator and a reference thermometer. The cold side of the thermocouples is held at the triple point of water using a triple point water cell. The whole experimental setup is controlled using LabView.

To determine the distribution of the two phases over the junction, the vapour qualities at the inlet and outlets of the junction have to be known. The vapour qualities cannot be measured but are calculated using the first law of thermodynamics. On average the absolute uncertainty on the vapour quality is always smaller than 0.02 and 0.02 for the inlet and the outlets, respectively.

$$x_b = \frac{h_{ob} - \frac{Q_{heater}}{\dot{m}_b} - h_{l,ib}}{h_{g,ib} - h_{l,ib}} \tag{3}$$

$$x_i = \frac{h_{ip} - \frac{Q_{preheater}}{\dot{m}} - h_{l,op}}{h_{g,op} - h_{l,op}} \tag{4}$$

To ensure valid data, the setup was first validated and tested. The law of conservation of mass over the junction was calculated. The overall deviation of the total mass flow rate was lower than $1\,\%$. Secondly, the first law of thermodynamics was computed over the whole setup. This energy balance closes with an error smaller than $3\,\%$ due to unaccounted heat transfer from the environment and due to measurement uncertainties. In order to assess the repeatability of the results, five random experiments were repeated on a different day. The results of the repetitions were all within the uncertainty of the original measurements.

3. RESULTS

3.1 Data Processing

In literature the results are often represented as the mass fraction of the liquid phase (F_l) that goes to one branch as function of the fraction of the vapour phase (F_g) that goes to the same branch. The same representation will be used in this work.

$$F_l = \frac{m_{l,b2}}{m_l} \tag{5}$$

$$F_g = \frac{m_{g,b2}}{m_g} \tag{6}$$

To find the main effects of the superficial velocities and saturation pressure on the distribution of R32 over an impacting T-junction, a full factorial experimental design was made. The full factorial design is shown in Table 2. For each row (a set of inlet conditions) in Table 2, the total mass fraction flowing to one branch was varied using needle valves. Hence, for each inlet condition, a graph of F_g as function of F_l was obtained. In total 133 measurements were obtained. Linear regression was used to determine a best fitting line of a set of measurements (an example can be seen in Fig. 3). The slope b of this line is also given in Table 2 with its 95% uncertainty interval. The flow regimes given in Table 2 are determined using the flow pattern map of Wojtan *et al.* (2005).

Table 2: Full factorial experimental design for determining the effects of the superficial vapour velocity, the superficial liquid velocity and the saturation temperature on the distribution of two-phase R32 over an impacting T-junction.

	T_{sat}	J_l	J_g	flow regime	$b\,(\alpha = 0.05)$
1	$10\,^{\circ}\mathrm{C}$	$0.2\,\mathrm{m/s}$	$1.5\,\mathrm{m/s}$	Intermittent	1.79 ± 0.06
2	$10\,^{\circ}\mathrm{C}$	$0.2\,\mathrm{m/s}$	$3\,\mathrm{m/s}$	Intermittent	1.28 ± 0.02
3	$10\,^{\circ}\mathrm{C}$	$0.3\,\mathrm{m/s}$	$1.5\,\mathrm{m/s}$	Intermittent	1.6 ± 0.1
4	$10\,^{\circ}\mathrm{C}$	$0.3\,\mathrm{m/s}$	$3\,\mathrm{m/s}$	Intermittent	1.38 ± 0.07
5	$20\,^{\circ}\mathrm{C}$	$0.2\,\mathrm{m/s}$	$1.5\,\mathrm{m/s}$	Intermittent	1.68 ± 0.04
6	$20\,^{\circ}\mathrm{C}$	$0.2\,\mathrm{m/s}$	$3\,\mathrm{m/s}$	Intermittent	1.25 ± 0.01
7	$20\,^{\circ}\mathrm{C}$	$0.3\,\mathrm{m/s}$	$1.5\,\mathrm{m/s}$	Intermittent	1.1 ± 0.1
8	$20\,^{\circ}\mathrm{C}$	$0.3\,\mathrm{m/s}$	$3\,\mathrm{m/s}$	Intermittent	1.39 ± 0.04
(9)	$10\,^{\circ}\mathrm{C}$	$0.2\,\mathrm{m/s}$	$5\,\mathrm{m/s}$	Annular	1.37 ± 0.02

The equation of the best fitting line is given by Eq. (7). In this work the straight line should pass through the point $(0.5; 0.5)$. If the total mass flow rate is divided equally over a symmetric T-junction, the the distribution is symmetrically i.e. F_g and F_l are both equal to 0.5 (Hwang *et al.*, 1989). This extra constraint leads to a relation between a and b given in Eq. (8).

$$y = a + b \cdot x \tag{7}$$

$$a = \frac{1-b}{2} \tag{8}$$

The regression line is fitted considering the uncertainties on the values of F_g and F_l. Based on the book of Bevington and Robinson (2003), the method of maximum likelihood is applied. The likelihood of the parameter b is given by Eq. (9).

$$P\left[b\right] = \prod_{i=1}^{n} \left[\frac{1}{\sqrt{2\pi\sigma_{x_i}^2}} \exp\left(-\frac{1}{2} \frac{\left(x_i - \mu_{x_i}\right)^2}{\sigma_{x_i}^2} \right) \frac{1}{\sqrt{2\pi\sigma_{y_i}^2}} \exp\left(-\frac{1}{2} \frac{\left(y_i - \frac{1-b}{2} - b\mu_{x_i}\right)^2}{\sigma_{y_i}^2} \right) \right] \tag{9}$$

The best fitting line maximises the likelihood $P[b]$. This is equivalent to finding the minimum of the sum in the exponential (Eq. (10)). The minimum is determined numerically using Matlab.

$$\chi^2 = \sum_{i=1}^{n} \left[\frac{\left(x_i - \mu_{x_i}\right)^2}{\sigma_{x_i}^2} + \frac{\left(y_i - \frac{1-b}{2} - b\mu_{x_i}\right)^2}{\sigma_{y_i}^2} \right] \tag{10}$$

Assuming that the likelihood function is a Gaussian function, the uncertainty on the parameter b is given by Eq. (11).

$$\sigma_b = \sqrt{2\left(\frac{\partial^2 \chi^2}{\partial b^2}\right)^{-1}} = \sqrt{2\left(\sum_{i=1}^{n}\left[\frac{2}{\sigma_{y_i}^2}\left(\mu_{x_i}^2 - \mu_{x_i} + \frac{1}{4}\right)\right]\right)^{-1}} \tag{11}$$

The b-values obtained with this analytical solution were compared with the ones found using the Monte Carlo method (n = 2 000 000). The deviation between the two results was negligible. The slope of the first experimental set found by the Monte Carlo method and the Maximum Likelihood method is respectively 1.78 ± 0.07 and 1.79 ± 0.06.

3.2 Analysis

First, the influence of the superficial vapour velocity (J_g) was investigated by comparing the experimental results for a varying J_g while keeping the superficial liquid velocity and saturation temperature constant. Figure 3 suggests that the slope decreases with increasing superficial vapour velocity. The same influence was found for the other experiments in Table 2, are significantly different. The slope decreases significantly if the superficial vapour velocity increases.

According to literature, an increasing inlet superficial vapour velocity J_g results in a decreased tendency of the liquid to exit through the outlet with the lowest mass flow rate. Translated to the rotation of a F_g-F_l graph, an increasing superficial vapour velocity leads to a clockwise rotation around the point (0.5;0.5) of the graph. Hence, the effect of J_g is similar as for water-air mixtures.

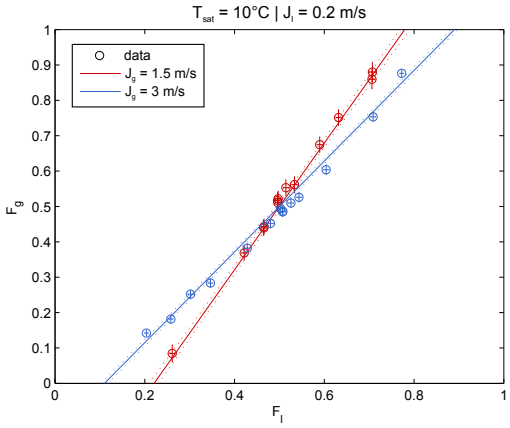

Figure 3: The vapour mass fraction as function of the liquid mass fraction for R32 divided over an impacting T-junction (T_{sat} = 10 °C; J_l = 0.2 m/s).

Second, the effect of the superficial liquid velocity (J_l) was investigated using the same method as for the superficial vapour velocity. Due to limitations of the experimental setup, the difference between the low and high superficial liquid velocity is rather small which makes the effects less pronounced as for the superficial vapour velocity. Figure 3 suggests an increasing slope with decreasing superficial liquid velocity when the superficial vapour velocity is low. Figure 4b suggests the opposite. The slope decreases with decreasing superficial liquid velocity when the superficial vapour velocity is high. These trends seen in Fig. 4 are confirmed by comparing the slopes in Table 2.

According to the results of the water-air experiments found in literature, the slope should increase with increasing superficial liquid velocity. In this work this is only found for high superficial vapour velocities. At low superficial vapour velocities the opposite behaviour was found.

An other difference with the water-air experiments is the occurrence of evaporation in the T-junction. Due to the pressure drop over the T-junction part of the liquid evaporates. This was mainly noticeable with higher mass fluxes.

Further, the influence of the flow regime was investigated. Figure 5 displays the results of experiment 1, 2 and 9 of Table 2. Normally should the slope decrease with increasing superficial vapour velocity. However, the slope of experiment 9 (annular flow) is larger than the one of experiment 2 (intermittent flow). This discontinuity between intermittent and annular flow was already observed by El-Shaboury *et al.* (2007) for water-air experiments.

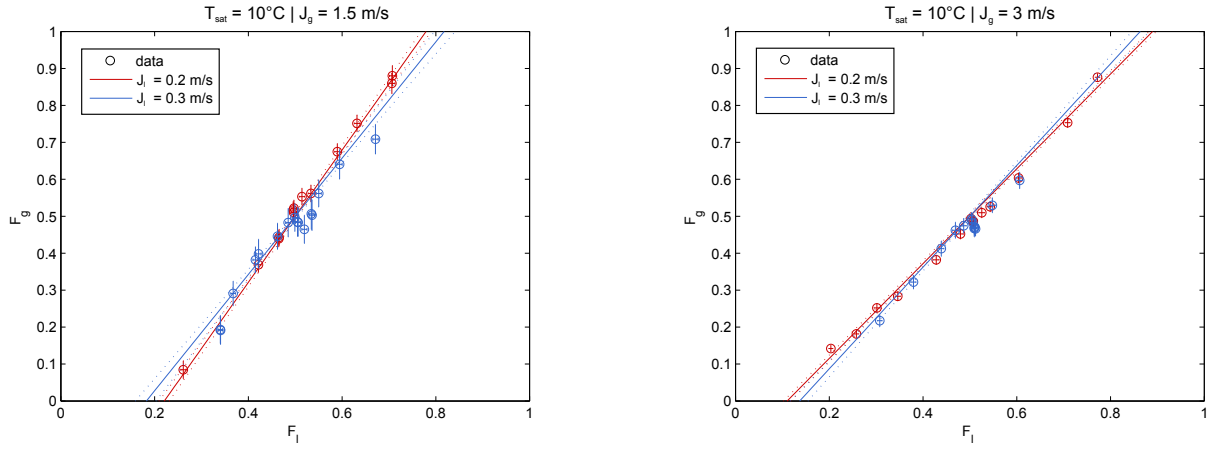

(a) $T_{sat} = 10\,^{\circ}\mathrm{C} \mid J_g = 1.5\,\mathrm{m/s}$ (b) $T_{sat} = 10\,^{\circ}\mathrm{C} \mid J_g = 3\,\mathrm{m/s}$

Figure 4: The vapour mass fraction as function of the liquid mass fraction for R32 divided over an impacting T-junction.

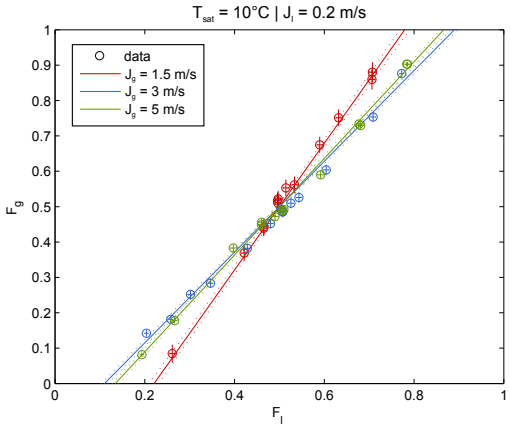

Figure 5: The vapour mass fraction as function of the liquid mass fraction for R32 divided over an impacting T-junction ($T_{sat} = 10\,^{\circ}\mathrm{C}$; $J_l = 0.2\,\mathrm{m/s}$).

Finally, the influence of saturation temperature, which is related to the pressure, was investigated. Figure 6 suggests that the effect of the saturation temperature is negligible. Comparing the slopes in Table 2 confirms this. However, the difference between the two measured saturation pressures is small (33%) due to the limitation of the experimental setup. In literature, authors found a small effect of pressure on the distribution of the two phases.

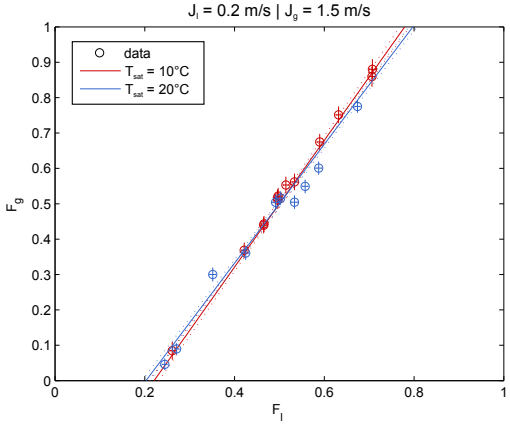

Figure 6: The vapour mass fraction as function of the liquid mass fraction for R32 divided over an impacting T-junction ($J_g = 1.5\,\mathrm{m/s}$; $J_l = 0.2\,\mathrm{m/s}$).

4. CONCLUSION

This experimental work studies the distribution of a two-phase refrigerant flow over a horizontal impacting T-junction. To conduct the experiments, an experimental setup was built which can test the distribution of two-phase mixtures (R32) at a saturation temperature between $10\,^{\circ}\mathrm{C}$ and $20\,^{\circ}\mathrm{C}$ with a mass flux of 150 to $700\,\mathrm{kg}/(\mathrm{m}^2{\cdot}\mathrm{s})$ and a vapour quality between 0 and 1.

Using design of experiments, the main effects of superficial vapour velocity, superficial liquid velocity and saturation temperature on the distribution of R32 were studied. For R32, the two phases only distribute uniformly over the T-junction when the mass flow rate through the two outlet branches is equal. Further, the experiments show a decreased tendency of the liquid to exit through the outlet with the lowest mass flow rate with increasing superficial vapour velocity. The opposite is noticed with an increasing superficial liquid velocity when the superficial vapour velocity is high. Further, during the experiments, evaporation occurs in the T-junction due to the pressure drop. Finally, no effect of the saturation temperature was found. Comparing with literature, one can conclude that not all main effects on the distribution of two-phase R32 are the same as for the water-air mixtures.

5. NOMENCLATURE

A	$[\mathrm{m}^2]$	cross-sectional surface area
COP	[-]	Coefficient Of Performance
D	$[\mathrm{m}]$	diameter
F	[-]	mass fraction
G	$[\mathrm{kg}/(\mathrm{m}^2{\cdot}\mathrm{s})]$	mass flux
h	$[\mathrm{W}/\mathrm{kg}]$	enthalpy
J	$[\mathrm{m}/\mathrm{s}]$	superficial velocity
$\dot{m}$	$[\mathrm{kg}/\mathrm{s}]$	mass flow rate
n	[-]	number of experiments
P	[Pa]	pressure
$P[\,]$	[-]	probability
Q	[W]	power
x	[-]	vapour quality

Special characters

ρ	$[\mathrm{kg}/\mathrm{m}^3]$	density

Subscripts

b	branch
g	gas phase
i	inlet
ib	inlet of parallel section
ip	inlet of preheater
l	liquid phase
ob	outlet of parallel section
op	outlet of preheater
sat	saturation

6. ACKNOWLEDGEMENTS

Research funded by a Ph.D. grant (nr. 141733) of the Agency for Innovation by Science and Technology (IWT)

7. REFERENCES

Azzopardi, B., Purvis, A., Govan, A. and Test, T., 1987. "Annular two-phase flow split at an impacting T". *International Journal of Multiphase Flow*, Vol. 13, No. 5, pp. 605–614. doi:10.1016/0301-9322(87)90038-3.

Bevington, P. and Robinson, D., 2003. *Data Reduction and Error Analysis for the Physical Sciences*. McGraw-Hill, 3rd edition. ISBN 9780072472271.

Chien, S. and Rubel, M., 1992. "Phase Splitting of Wet Steam in Annular Flow Through a Horizontal Branching Tee". *SPE Production and Facilities*, Vol. 7, No. 4, pp. 368–374. doi:10.2118/28542-PA.

De Kerpel, K., Ameel, B., De Schampheleire, S., T'Joen, C., Canière, H. and De Paepe, M., 2014. "Calibration of a capacitive void fraction sensor for small diameter tubes based on capacitive signal features". *Applied Thermal Engineering*, Vol. 63, pp. 77–83. doi:10.1016/j.applthermaleng.2013.11.006.

De Kerpel, K., De Schampheleire, S., De Keulenaer, T. and De Paepe, M., 2015. "Two-phase flow regime assignment based on wavelet features of a capacitance signal". *International Journal of Heat and Fluid Flow*, Vol. 56, pp. 317–323. doi:10.1016/j.ijheatfluidflow.2015.09.002.

El-Shaboury, A.M.F., Soliman, H.M. and Sims, G.E., 2007. "Two-phase flow in a horizontal equal-sided impacting tee junction". *International Journal of Multiphase Flow*, Vol. 33, No. 4, pp. 411–431. doi: http://dx.doi.org/10.1016/j.ijmultiphaseflow.2006.10.002.

European Commission, 2017. "Buildings - european commission". URL `https://ec.europa.eu/energy/en/topics/energy-efficiency/buildings`. [Online; accessed 6-March-2017].

Hong, K. and Griston, S., 1995. "Two-Phase Flow Splitting at an Impacting Tee". *SPE Production & Facilities*, Vol. 10. doi:10.2118/27866-PA.

Hwang, S.T., Soliman, H.M. and Jr, R.T.L., 1989. "Phase separation in impacting wyes and tees". *International Journal of Multiphase Flow*, Vol. 15, No. 6, pp. 965–975. doi:http://dx.doi.org/10.1016/0301-9322(89)90024-4.

Lightstone, L., Osamusali, S.I. and Chang, J.S., 1991. "Gas-liquid two-phase flow in symmetrically dividing horizontal

tubes". *AIChE Journal*, Vol. 37, No. 1, pp. 111–122. doi:10.1002/aic.690370110.

Mader, G., Palm, B. and Elmegaard, B., 2015. "Maldistribution in air-water heat pump evaporators. Part 1: Effects on evaporator, heat pump and system level". *International Journal of Refrigeration*, Vol. 50, pp. 207–216. doi:10.1016/j.ijrefrig.2014.07.006.

Mohamed, M., Soliman, H. and Sims, G., 2011. "Experimental investigation of two-phase flow splitting in an equal-sided impacting tee junction with inclined outlets". *Experimental Thermal and Fluid Science*, Vol. 35, No. 6, pp. 1193–1201. doi:10.1016/j.expthermflusci.2011.04.006.

Mohamed, M., Soliman, H. and Sims, G., 2014. "Effects of pipe size and system pressure on the phase redistribution in horizontal impacting tee junctions". *Experimental Thermal and Fluid Science*, Vol. 54, pp. 219–224. doi:10.1016/j.expthermflusci.2013.12.019.

Nakayama, M., Sumida, Y., Hirakuni, S. and Mochizuki, A., 2000. "Development of a refrigerant two-phase flow distributor for a room air conditioner". *International Refrigeration and Air Conditioning Conference*.

Ottens, M., De Swart, A., Hoefsloot, H. and Hamersma, P., 1995. "Gas-Liquid Flow Splitting in Regular, Reduced and Impacting T Junctions." *Impiantistica Italiana*, Vol. 8, No. 2, pp. 26–37.

Wojtan, L., Ursenbacher, T. and Thome, J.R., 2005. "Investigation of flow boiling in horizontal tubes: Part IâĂŤA new diabatic two-phase flow pattern map". *International Journal of Heat and Mass Transfer*, Vol. 48, No. 14, pp. 2955–2969. doi:10.1016/j.ijheatmasstransfer.2004.12.012.

Yoshioka, S., Kim, H. and Kasai, K., 2008. "Performance Evaluation and Optimization of A Refrigerant Distributor for Air Conditioner". *Journal of Thermal Science and Technology*, Vol. 3, No. 1, pp. 68–77. doi:10.1299/jtst.3.68.